Construction and Building Materials 427 (2024) 136215

Contents lists available at ScienceDirect

Construction and Building Materials

journal homepage: www.elsevier.com/locate/conbuildmat

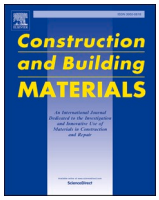

Estimation by capillary water absorption method to building natural stones' durability against freeze-thaw

Jose Vercher [a,*], Júlia G. Borràs [a], Carlos Lerma [a], Ángeles Mas [a], Enrique Gil [b]

[a] Dpt. Architectural Constructions, Universitat Politècnica de València, Camino de Vera s/n, Valencia 46022, Spain
[b] Dpt. Architectural Structures, Universitat Politècnica de València, Camino de Vera s/n, Valencia 46022, Spain

ARTICLE INFO

Keywords:
Natural building stone
Freeze-thaw
Capillary water absorption
Porosity
Durability estimation

ABSTRACT

In construction, the proper selection of natural building stones and the prediction of their pathology are significant, with freeze-thaw action being a primary cause of deterioration. Testing for freeze-thaw durability, being labour-intensive and time-consuming, often conflicts with construction timelines. The proposed methodology estimates natural stone behaviour against frost damage using quicker laboratory tests (e.g., capillary water absorption). The use of natural stones with an open porosity exceeding 2 % is not advisable, as exceeding this threshold leads to losses in compressive strength of more than 10 % after 168 freeze-thaw cycles. This alternative evaluation through the capillary water absorption method provides a precise estimation of freeze-thaw durability, proving to be an instrumental tool for architects when selecting natural stones.

1. Introduction

Natural building stones are extensively utilised in the field of architecture, offering a wide array of choices with substantial differences in intrinsic and mechanical properties, durability, and applications.

One of the primary factors impacting the long-term durability of exterior building stone installations is Freeze-Thaw (FT) action [1]. When water freezes within stone pores, it initially increases the liquid water volume by 9 %, raising both volume and pressure at lower freezing temperatures [2]. Freezing initiates in larger pores and redistributes to adjacent ones if there is insufficient space for ice formation locally [1,3,4]. Notably, not all water freezes at the same temperature, with the freezing point of pore water decreasing with pore size [5–8]. Water in pores between 100 μm and 1000 μm, for instance, does not freeze until around −20 ℃ due to interfacial free energy effects [4,9,10]. Conversely, water freezes at higher temperatures in larger pores, resulting in more significant frost damage. Factors such as the initial stone saturation coefficient also play a role, as higher saturation percentages lead to greater stone deterioration [2].

As the pressure exerted by this volume and the migration of unfrozen water increase and reach the tensile strength of the stone, new microcracks appear and existing ones deepen [4,6,11]. Repeated FT cycles lead to material weakening, resulting in reductions in uniaxial compression strength [12,13], increased porosity [14], weight loss [15], alterations in colour [16], exfoliation, and the formation of surface layers [17], among other effects.

Several intrinsic stone properties, such as mineralogical composition, grain size, and porosity, are interconnected with the functional properties relevant to their architectural applications. These properties describe how the stone responds to environmental conditions, including mechanical loads and FT cycles [18]. The vulnerability of a stone to ice damage is influenced by various factors, including initial saturation [6,19–21], the number of cycles, temperature, and applied stress [6,22]. Moreover, intrinsic properties like open porosity, pore size distribution, grain size, and capillary water absorption significantly impact FT weathering [23–30].

This suggests that intrinsic properties can serve as indicators for assessing the functional characteristics of the stone [18,31]. The objective of this research is to estimate the performance of 14 types of natural stones (Fig. 1) against FT cycles based on various intrinsic properties. Several studies have shown that the stone type (textural properties) alone does not provide comprehensive insights into durability against FT cycles [1,3,23]. However, previous research has not conducted a comprehensive examination of the behaviour against FT cycles of principal building natural stones, typically concentrating on a singular family in each instance. It is acknowledged that natural stones sourced from the same origins can exhibit significant variations in porosity and other textural attributes [32]. Nonetheless, a comparative

* Corresponding author.
E-mail address: jvercher@csa.upv.es (J. Vercher).

https://doi.org/10.1016/j.conbuildmat.2024.136215
Received 24 November 2023; Received in revised form 4 February 2024; Accepted 8 April 2024
Available online 17 April 2024

study encompassing diverse stone families is essential. This paper facilitates the comparison of durability against frost damage among the primary natural stones, enabling an evaluation of their behaviour through the same methodology. The suitability of each stone for exterior applications, considering the potential for frost damage, is evaluated based on the capillary water absorption method, which considers textural properties, open porosity, and compressive strength.

Moreover, the necessity to adhere to stringent construction schedules is often not included when professional architects evaluate the methods for assessing the suitability of various building materials. Specifically, the freeze-thaw test is exceedingly time-intensive (requiring samples for 84 days in a climatic chamber with 2 cycles per day) [12,33]. The development of a methodology that is both time-efficient and capable of delivering pertinent and precise data regarding the freeze-thaw durability of natural stones would significantly broaden the applicability and expedite the utilisation of this information in the construction sector.

2. Materials and methods

The methodology developed in this study aims to provide valuable assistance to architectural professionals when selecting natural stones for exterior areas exposed to rain and frost. The primary objective of this research is to predict how different natural stones will behave in the presence of frost using alternative laboratory tests that can be completed within a few hours.

Fourteen distinct natural stones have been examined, covering the principal groups commonly used in architectural construction (Fig. 1). Table 1 presents the commercial names of these 14 stones, along with their classifications and textural properties. Petrographical characteristics provide insights into the origin and formation of each stone, proving invaluable in the study and prediction of their durability against environmental agents [26]. Among the samples, 14.3 % are igneous rocks (A-B), 50 % are sedimentary rocks (C-I), and 35.7 % are metamorphic rocks (J-N). Within the sedimentary category, 42.9 % are sandstone, 14.3 % are lumachelle limestone, 28.5 % are limestone, and 14.3 % are alabaster. These 14 varieties of natural stone have been sourced from renowned Spanish quarries that are prominent at both national and international levels: Levantina (A-B-H-I-J-K-M-N), Olnasa (C-D-E-F), Arastone (G), and Cupa Pizarra (L). Each of these companies has provided a minimum of 9 samples for each stone, which have been identified with a corresponding letter and consecutive numbering. All samples are cubic, measuring 50 ± 5 mm per side, adhering to the standards' requirements for capillary water absorption, FT, and uniaxial compressive strength tests. All finished surfaces have been sawn.

Out of the 9 samples, three were utilised to determine their physical properties through laboratory tests, following the UNE-EN 1936:2007 standard [34]. The physical properties examined include real and bulk density, open and total porosity, and compactness of each stone. The actual density values represent the average obtained from the results of three samples for each stone. These samples were not employed for other tests due to the nature of the procedure.

Subsequently, the capillary water absorption test, in accordance with the UNE-EN 1925:1999 standard [35], was conducted. This test, which is simple, swift, and cost-effective, forms the methodological foundation of this research for estimating frost damage, in conjunction with the determination of other intrinsic properties. Six samples of each stone were subjected to this test. These samples were immersed in a tank after being dried to a constant mass, with the water level set at 3 ± 1 mm. Weighing was performed at nine intervals: 1, 3, 5, 10, 15, 30, 60, 480, and 1440 minutes (24 hours). According to Ozcelik and Ozguven [36], the first 24 hours are critical in terms of water absorption. The capillary absorption coefficient (C) was determined, and the results are presented in Fig. 2 in the form of a graph, illustrating the absorption coefficient (g/m^2) plotted against the square root of time ($\sqrt{t}$). The average values, calculated from the results obtained for the six samples, were used for analysis.

Lastly, the FT test is designed to replicate stress conditions typically caused by the absorption of water and its subsequent freezing within the stone's capillary network. These mechanisms can induce both superficial and internal damage to the stone, altering its physical and mechanical properties, as well as degrading its aesthetic features. Once the capillary water absorption for each stone is established, its durability to FT cycles is analysed in accordance with UNE-EN 12371:2011 [37]. Of the six available samples (e.g., A1-A2-A3-A4-A5-A6), three (e.g., A1-A2-A3) undergo the FT test to assess the resultant damage. An additional set of three fresh samples (e.g., A4-A5-A6) is utilised to determine the uniaxial compressive strength prior to the FT cycles, in line with UNE-EN 1926:2007 [38] (using the Ibertest MEH series compression testing machine, 1500 kN version).

Each FT cycle spans 12 hours and involves three samples. Initially,

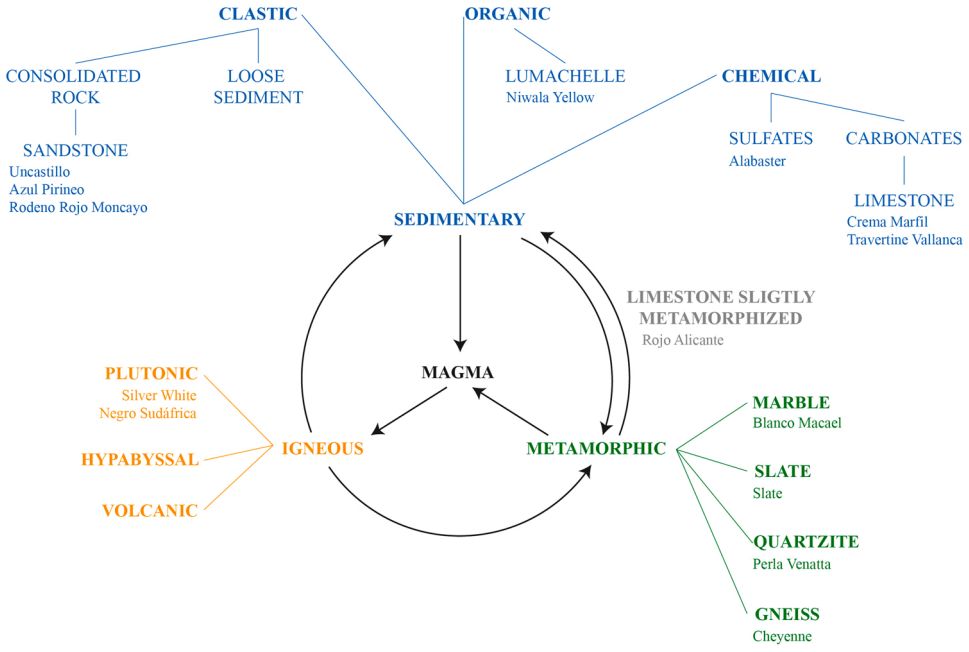

Fig. 1. Classification of the 14 types of stones under investigation.

Table 1
Name, classification, and textural properties of the studied natural stone samples.

	STONE NAME	STONE CLASSIFICATION	TEXTURAL PROPERTIES
A	Silver White	Leucocratic plutonic; Granite	Massive and grainy stone, medium grain size (phaneritic rock). Low-porosity building stone.
B	Negro Sudáfrica	Melanocratic plutonic; Gabbro	Massive and grainy uniform composition, fine-medium grain size (phaneritic rock), and high compactness.
C	Uncastillo	Carbonate Sandstone; Lithic sandstone	Clastic sedimentary rock, fine-grained (average particle diameter 150 μm). Clean sandstone (free of matrix).
D	Azul Pirineo	Carbonate Sandstone; Lithic sandstone	Clastic sedimentary rock, fine-grained (average particle diameter 100 μm). Clean sandstone (free of matrix).
E	Rodeno Rojo Moncayo	Siliceous sandstone; Feldspathic wacke	Clastic sedimentary rock, with a phyllosilicate matrix, and foliated. The average size of quartz clasts is 0.18 mm, and feldspar is 0.13 mm. Low-porosity building stone.
F	Niwala Yellow	Lumachelle limestone	Calcareous-bioclastic sedimentary rock, of marine origin. Clastic structure, with high porosity.
G	Alabaster	Gypsum	Massive variety of gypsum composed of fine-grained crystals, translucent and soluble in water.
H	Crema Marfil	Litographic limestone	Carbonate sedimentary rock, fine grain size (0,01–2 mm), and granular massive texture.
I	Travertine Vallanca	Travertinic limestone	Carbonate sedimentary rock, fine grain size, and abundant fenestral porosity (irregular, size 0,01–10 mm).
J	Rojo Alicante	Limestone slightly metamorphized	Metamorphism of carbonate sedimentary rocks, slightly metamorphized. Fine-grained, low porosity, and vermilion with white calcite recrystallized veins distributed irregularly.
K	Blanco Macael	Calcitic marble	Metamorphism of carbonate sedimentary rocks. Compact and granular structure (recrystallization), homogeneous, and low porosity.
L	Slate	Slate	Metamorphism of sedimentary rocks composed of clay. Compact and foliated structure, fine-grained, and low porosity.
M	Perla Venatta	Quartzite	Metamorphism of sedimentary rocks, sandstone. Compact and massive structure, fine-medium grain size, and low porosity.
N	Cheyenne	Gneiss	Metamorphism of igneous plutonic rocks, granite. Schist and banded gneiss. Medium-grained and low porosity.

the samples were saturated by immersion in water within the climatic chamber (Model: Controls CCK 480; Temperature range: −25 °C to 150 °C; Humidity range: 15–98 % RH, as per the psychrometric chart). These samples were then frozen for 6 hours, attaining minimum temperatures in the core of independently monitored samples (Fig. 3) ranging between −8 and −12 ℃, adhering to the standards set forth [37] (Fig. 4). Following this, the samples were thawed to a temperature not exceeding 20 ℃ and subsequently re-saturated. Both the filling and draining system of the container holding the samples within the climatic chamber and the temperature controls have been automated, enabling the execution of two FT cycles every 24 hours.

For the samples subjected to the FT test, various parameters are analysed after 14, 56, 84, 140, and 168 cycles. These parameters include dry weight, saturated weight, submerged saturated weight, bulk density, P-wave velocity, and visual inspection. In context to the number of cycles, Martínez-Martínez et al. [39] recommend a minimum of 100 FT cycles to yield conclusive data.

The day following each set of cycles, the saturated and submerged saturated weights of the samples are determined. This is followed by a 24-hour drying period to ascertain the dry weight, enabling the performance of ultrasonic measurements and visual inspections. Although ultrasonic testing is not a standard requirement for evaluating the state of decay, monitoring the weathering process of the samples via ultrasonic measurements has been extensively employed in numerous studies to augment the available data [5,21,39–46]. The P-wave velocity, as determined by these measurements, provides insights into the varying degrees of compactness as the cycles progress. This change in compactness may correlate with the development of microcracks, reduced continuity of the solid material, and losses in mechanical strength. The portable ultrasonic tester used in this study is a Steinkamp BP-5 equipped with 50 kHz exponential tip sensors.

Subsequently, the samples undergo a saturation process for a minimum of 6 hours prior to the commencement of the new FT cycle. Prior to this, a detailed study was conducted to ascertain the requisite drying and saturation times for a sample of each stone type. This study concluded that all stones required no more than 24 hours for drying and 6 hours for saturation. At the conclusion of the testing period, the uniaxial compressive strength of the samples is also determined after undergoing 168 FT cycles.

3. Results and discussion

Table 2 provides a summary of the principal values derived from the various tests conducted in this research. The data presented in the table represent average values from the tests performed on either 3 or 6 samples, as specified in the notes. With the exception of instances outlined in the table, the coefficient of variation (CV) remains below 30 % (0.3).

As indicated in Table 2, the capillary water absorption test and the FT test, along with the measurements of open porosity and compactness, have not been conducted for the alabaster samples (G). Alabaster, being a water-soluble stone material primarily composed of $CaSO_4$ 2 H_2O, exhibits mass loss when submerged. Consequently, it is determined that alabaster is not a suitable material for exterior installation, where it is likely to undergo mass losses owing to the solubility of its constituents.

Fig. 5 includes an outline illustrating the methodology proposed in this study.

3.1. Open porosity and capillary water absorption

Fig. 6 depicts the various stones, arranged in order of increasing open porosity. This research has revealed that when total water absorption values are considered, the ranking remains largely consistent with that of capillary water absorption. It is observed that a higher open porosity, typically indicative of greater total porosity, correlates with increased capillary water absorption noted at 24 hours. For open porosity values less than or approximately 2 %, there is a modest rise in water absorption, with values ranging from 100 g/m^2 to 600 g/m^2.

These analyses underscore the variability in properties and characteristics that sandstones (C-D-E) can exhibit, depending on intrinsic properties such as grain size or the cementing materials. Notably, in this instance, the sandstone with the lowest open porosity and water absorption is sample D (Azul Pirineo), which possesses the smallest average grain size.

3.2. Open porosity and loss of compressive strength

Fig. 7 illustrates the relationship between the values of open porosity and the reduction in compressive strength following the FT cycles. The

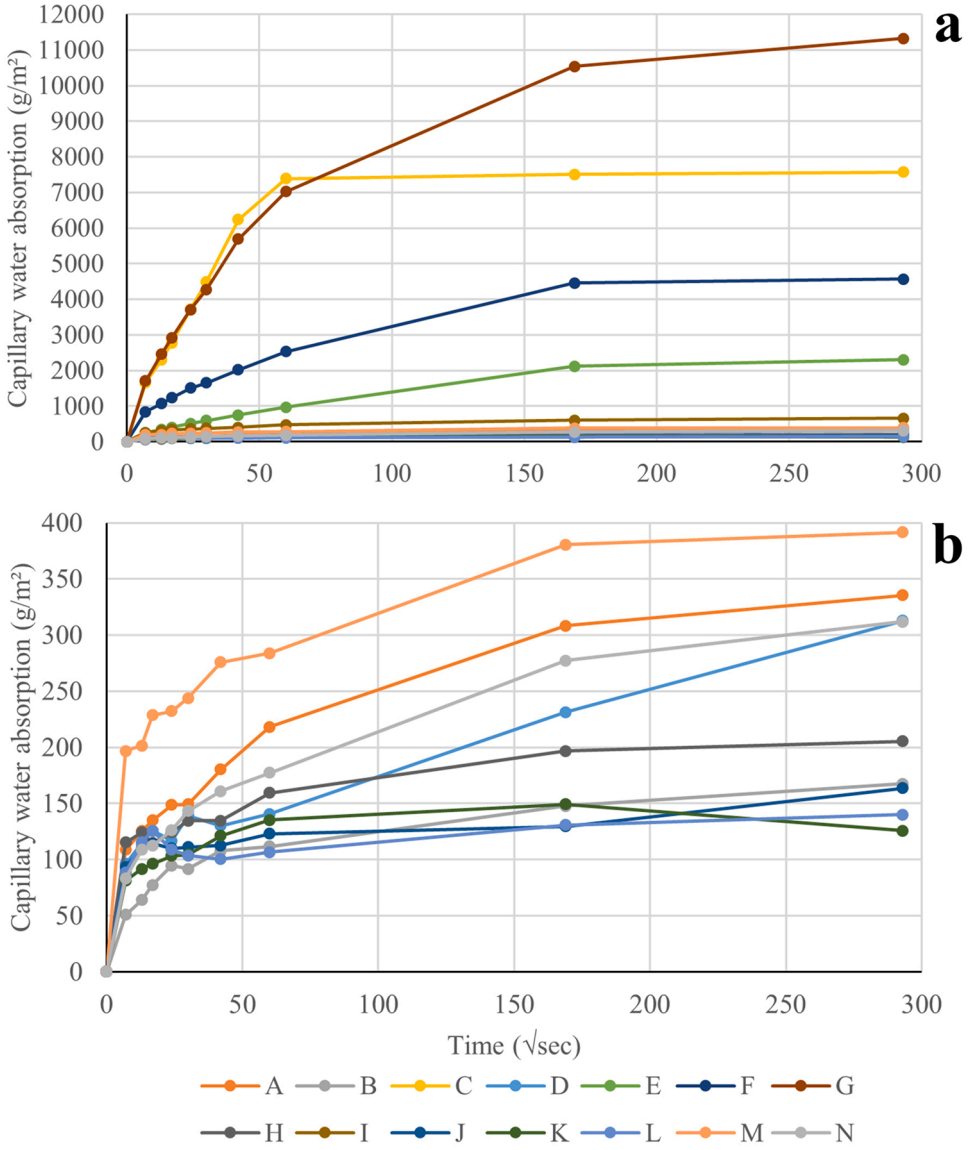

Fig. 2. (a) Average capillary water absorption (g/m^2) for each time interval (√sec) of each stone; (b) Only the stones with capillary water absorption at 24 hours less than 500 g/m^2.

graph suggests that materials characterised by lower porosity values, typically indicative of greater compactness, tend to exhibit a diminished reduction in compressive strength.

For this graph, the loss of compressive strength (R_{closs}) is calculated based on the compressive strength of the fresh samples (R_{c0}) and the samples after 168 FT cycles (R_{c168}). However, the compressive strength of natural stones is influenced by their bulk density, with higher bulk density typically resulting in greater compressive strength for the same pore volume. Consequently, a preliminary study has been conducted on the R_c/ρ_b coefficient of both fresh samples and those after 168 FT cycles. By comparing these coefficients, rather than the strength values, potential errors arising from samples that may exhibit higher compressive strength due to increased bulk density are mitigated. The comparative analysis of these coefficients (R_c/ρ_b) reveals a similar pattern to that observed when examining the value of compressive strength loss after the FT test (Rc_{loss}), thereby validating the use of the R_{closs} values for drawing conclusions.

Specifically, it is noted that for open porosity values less than 2 % ($C > 0.93$), a loss in compressive strength after 168 cycles is recorded at zero or below 10 % in most instances. In cases where the loss of compressive strength (A-H-M) is not indicated, an increase in compressive strength has been observed after 168 FT cycles. It is important to acknowledge that stones are natural materials, and as such, the potential variability in characteristics and properties is inherent to their very nature. Numerous studies investigating the effects of water absorption and weathering due to FT cycles have reported varied and sometimes contradictory results, attributable to this inherent variability of natural materials [47].

The aforementioned trend is not observed in the slate samples (L), which can be attributed to the textural properties of this stone. Slate, with its foliated structure, features minerals arrayed in thin layers. This composition results in superior bending behaviour compared to compressive strength, in contrast to other stone materials. Due to this characteristic, the losses in compressive strength following FT cycles in slate are proportionally greater relative to their initial values than in other massive building stones with similar open porosity. Additionally, despite being a natural stone with low porosity, water accumulation and distribution in slate are predominantly concentrated between the different layers. After FT cycles, an increase in porosity and microcracks at specific points between the layers leads to a considerable reduction in compressive strength.

Another studied stone with a foliated structure is the rodeno rojo

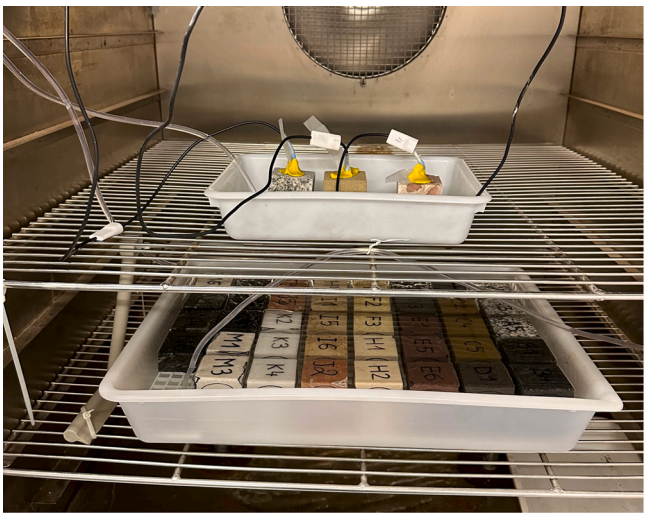

Fig. 3. Monitoring of temperatures in independent samples at the top and saturation tray at the bottom.

Moncayo sandstone (E). In this case, the E samples exhibit a loss of compressive strength of 15.11 %, aligning with an open porosity exceeding 2 %. Although this stone contains schists, its cementing material is siliceous. The composition of the matrix (cementation type) significantly impacts the degree of deterioration after FT cycles in sandstones [40,48]. For the E stone, the siliceous cementing material provides enhanced mechanical strength, resulting in lower losses of compressive strength after FT cycles compared to slate.

It is also observable that the larger the porosity size in stones, the more significant is the decline in compressive strength following the FT cycles. In this context, the most substantial losses of compressive strength are seen in samples I (Travertine Vallanca) and F (Niwala Yellow). Owing to their formation and textural properties, both of these natural stones exhibit larger porosity compared to other samples. This larger porosity facilitates the attainment of freezing temperatures within the pores, and the subsequent volume expansion due to ice crystallization generates high internal tensions. These tensions are responsible for the formation of microcracks, the reduction of mechanical strength, and even superficial damage to the stone. Conversely, in samples H (Crema Marfil), there is no loss of compressive strength. This is attributed to the fine grain of the stone and its massive granular texture, resulting in a very fine capillary network. The durability of these samples under FT cycles is higher, despite exhibiting water absorption values similar to other building stones with comparable open porosity (J). As Rusin et al. [27] indicate, fine-grained stones tend to offer more optimistic predictions than coarse-grained stones, as they possess smaller pores, which in turn lower the freezing temperature.

3.3. Capillary water absorption and freeze-thaw

During the FT test, to which three samples of each stone type were subjected, various properties were analysed after specific numbers of cycles, with P-wave velocity and visual inspection being particularly noteworthy. Initially, P-wave velocity (v_p) was ascertained by calculating the ratio of the sample's length to the pulse transit time [46]. This metric provides insights into potential internal damage or deterioration of the samples that might not be apparent during visual inspection, yet could impact the stone's mechanical strength (e.g., microcracking, increased porosity, reduced compactness). As depicted in Fig. 8, it is generally observed that most samples exhibit a decrease in v_p, suggesting a potential reduction in compactness due to internal microcracks or an increase in porosity [49]. This reduction implies a loss of mass at the same volume and discontinuities in the stone's internal structure, leading to diminished compressive strength after the FT cycles.

Some samples, however, demonstrate an increase in v_p after 168 FT cycles. It must be noted that, given the natural material's inherent nature, predicting its behaviour invariably involves exceptions and potential errors in the ultrasonic test, which could stem from the precision of the testing device or the sample's relatively short length (approximately 50 mm). The natural variability of stones is distinctly evident in the v_p of samples K and N. Despite originating from the same quarry, these samples exhibit varied v_p values, indicating differences in their bulk density, porosity, and compactness.

Simultaneously, the evolution of the compactness of the tested samples has been meticulously evaluated. Fig. 9 delineates this progression throughout the FT cycles. As anticipated and corroborated by the ultrasound evolution analysis, natural stones exhibit deterioration commensurate with an escalation in the number of FT cycles. This decline is predominantly acute within the initial 14 cycles. However, as has been reiterated in this document, owing to the inherent lack of homogeneity in these natural materials, individual samples may exhibit variances. This general tendency does accommodate certain anomalies,

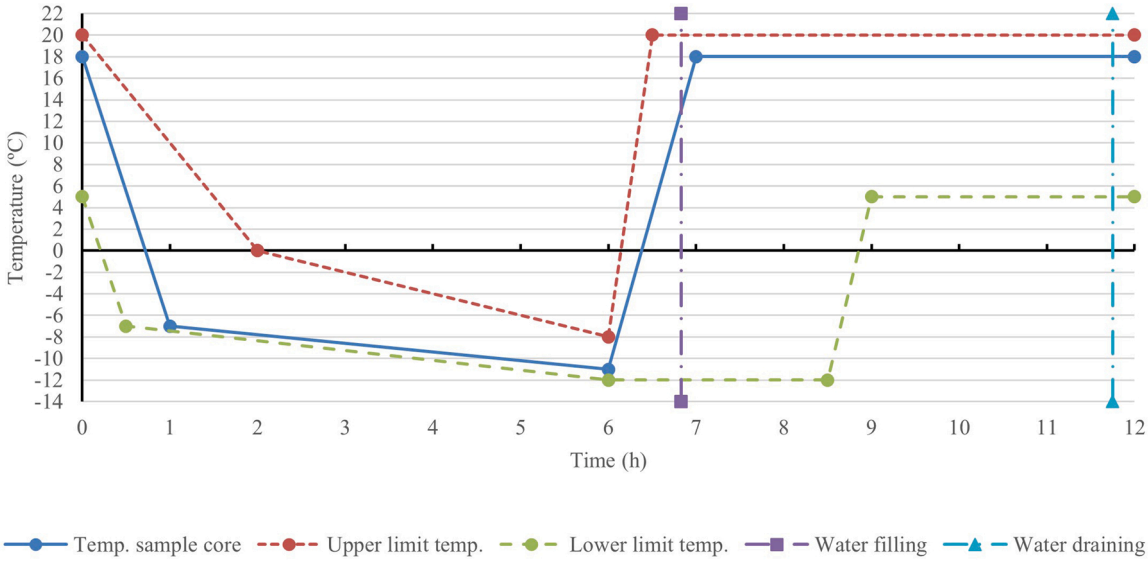

Fig. 4. Control of the water-filling process and monitoring of the core temperatures of the samples during the freeze-thaw cycle, in compliance with the standard UNE-EN 12371:2011.

Table 2
Initial real density, ρ_r (g/cm^3); initial bulk density, ρ_b (g/cm^3); initial compactness, C (%); initial open porosity, n (%); initial compressive strength, R_{c0} (MPa); compressive strength after 168 freeze-thaw cycles, R_{c168} (MPa); compressive strength loss after 168 freeze-thaw cycles in relation to initial values, R_{closs} (%); coefficient initial compressive strength/initial bulk density coefficient, R_{c0}/ρ_{b0}; coefficient compressive strength after 168 cycles/bulk density after 168 cycles, R_{c168}/ρ_{b168}; capillary water absorption after 24 hours, A (g/m^2).

	ρ_r[a]	ρ_b[b]	C	n[b]	R_{c0}[a]	R_{c168}[a]	R_{closs}	R_{c0}/ρ_{b0}[a]	R_{c168}/ρ_{b168}[a]	A[b]
A	2.64	2.60	98.48	0.92	145.35	156.91	-	5633.2	6123.1	335.37
B	3.01	2.94	97.67	0.57	260.99	232.61	10.87	9101.2	8128.3	167.32
C	2.60	2.11	81.15	15.08	34.60	27.39	20.85	1660.8	1322.5	7568.19
D	2.67	2.62	98.13	1.73	106.60	99.52	6.64	4065.4	3803.4	312.70
E	2.67	2.44	91.39	4.75	118.28	100.41	15.11	4860.6	4133.7	2301.88
F	2.63	2.25	85.55	9.36	55.96	38.56	31.09	2485.2	1754.4	4560.31
G	2.72	2.34	-	-	-	-	-	-	-	-
H	2.64	2.66	100.00[c]	0.83	150.87	179.78	-	5688.0	6763.5	205.35
I	2.68	2.48	92.54	2.41	91.83	58.74[d]	36.04	3723.8	2466.8	654.98[d]
J	2.68	2.65	98.88	0.79	137.03	125.81	8.18	5143.4	4746.7	163.50
K	2.70	2.67	98.89	0.42	80.14	74.32	7.27	2999.6	2776.4	125.63
L	2.81	2.80	99.64	0.52	240.14	186.66	22.27	8615.8	6689.6	139.93
M	2.73	2.57	94.14	1.44	126.65	130.28[e]	-	4883.6	5008.0	391.51[e]
N	2.89	2.70	93.43	1.05	173.47	164.92	4.93	6455.4	6150.6	311.90

[a] Average value of 3 samples.
[b] Average value of 6 samples.
[c] A value exceeding 100 % is observed because the bulk density surpasses the real density. This result is implausible and is likely attributable to errors stemming from the test procedure itself, such as the surface drying of the saturated samples, combined with the high precision of the balance (0.01 g).
[d] The CV is approximately 0.5. This variation can be attributed to the intrinsic formation process of travertine, which involves the precipitation of carbonated waters on algae. Over time, these algae biodegrade, resulting in a notably heterogeneous porosity within the stone. Consequently, this leads to a greater dispersion in the test results across different samples.
[e] The CV stands at 0.38. This result is likely attributable to errors stemming from the test procedure itself, such as the surface drying of the saturated samples, combined with the high precision of the balance (0.01 g).

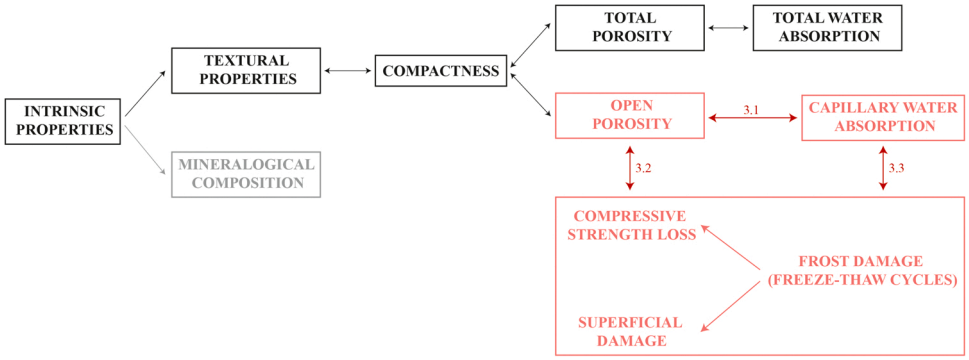

Fig. 5. Outline of the proposed methodology.

such as those observed in Perla Venatta (M) and Crema Marfil (H).

Regarding the visual inspection conducted after the FT cycles, no apparent surface degradation was observed in most of the stones studied. Prior to the FT test, any pre-existing breaks, cracks, or damage on all the tested samples were marked. After completing 168 cycles, only samples I1 and I3 (Travertine Vallanca) exhibited visible damage on their surfaces and edges. Sample I1 showed minor damage, characterized by the rounding of one of its corners, yet this did not compromise the sample's overall integrity. In contrast, I3 exhibited more significant damage, including the breakage of one of its corners (fragment > 30 mm^2), along with notable signs of disaggregation. This damage can be attributed to the stone's capillary network or porosity size. In the case of travertine, its formation process, involving the precipitation of carbonated waters on algae, results in a porosity with variable distribution and size. Water in the larger pores freezes at a higher temperature, leading to more pronounced damage during the FT cycles. The travertine samples subjected to FT cycles, despite being sourced from the same quarry, had large and highly variable porosity. This variability is reflected in the differing degrees of visual deterioration observed among the samples: no visible deterioration in I2, minimal damage in I1, and significant degradation in I3.

From an architectural standpoint, it can be concluded that the visual appearance of most natural stones does not undergo significant degradation after 168 FT cycles. However, stones with a larger capillary network and irregularly distributed porosity are more prone to developing cracks, holes, or breaks, which can visually degrade the stone. Therefore, the use of stones like travertine in exterior applications should be avoided or restricted to pieces where the porosity has been filled with resins or other durable lime-based materials.

In terms of uniaxial compressive strength, it has been established that stones with higher capillary water absorption tend to suffer greater losses in compressive strength after undergoing 168 FT cycles. Consequently, the use of stones with an open porosity exceeding 2 % in exterior applications is not advisable, especially in conditions susceptible to frost damage. The estimation of stone's behaviour against FT cycles through capillary water absorption tests and porosity studies is validated by these findings. These tests are more time and cost-efficient compared to the FT test and provide reliable information about the mechanical compressive behaviour of natural stones by analysing their capillary water absorption and open porosity.

It merits emphasis that this investigation was unable to procure definitive outcomes for alabaster (G), attributing to the samples undergoing mass diminution during the tests as a consequence of the solubility of its components. Notwithstanding this, while alabaster is

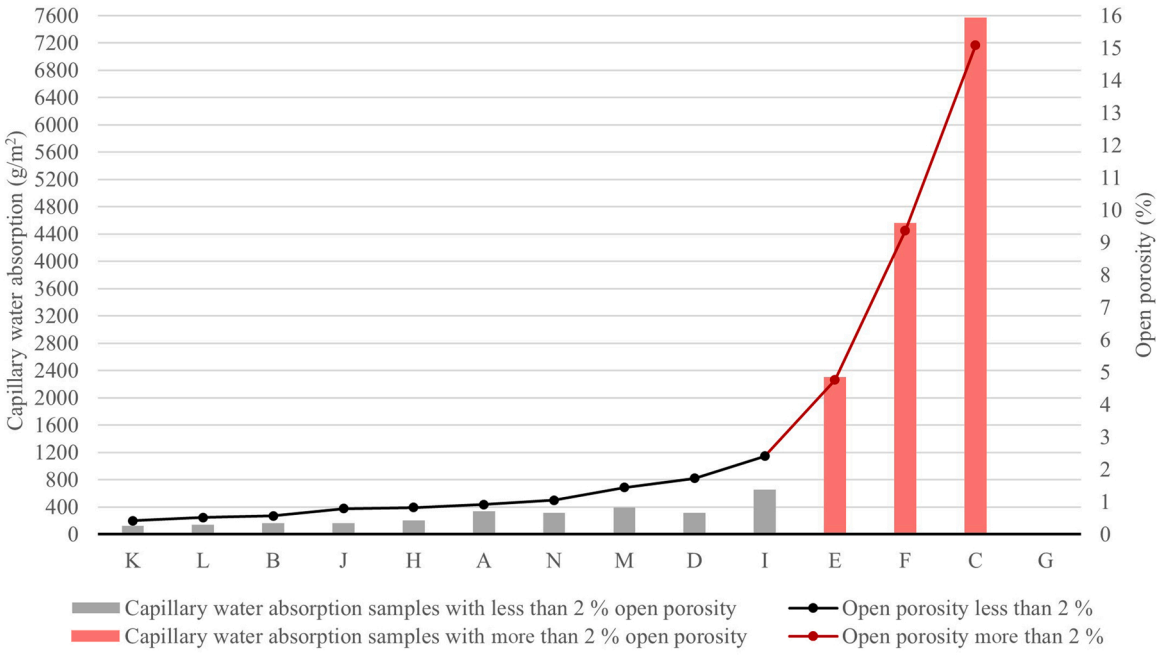

Fig. 6. Relationship between capillary water absorption after 24 h (g/m^2) and open porosity (%).

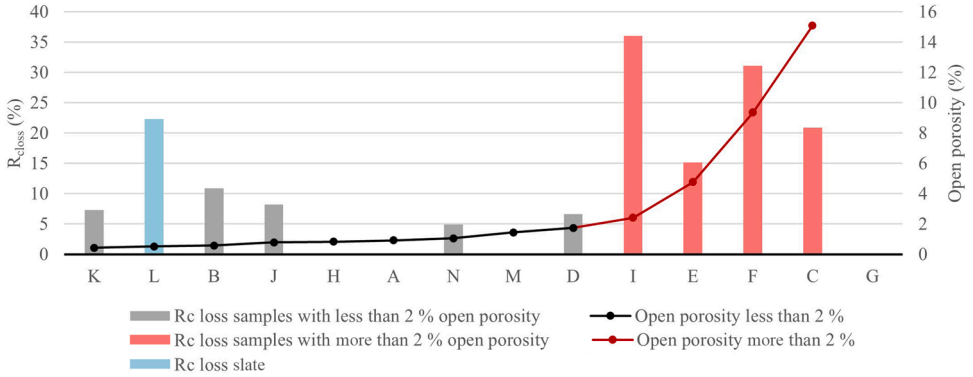

Fig. 7. Relationship between reduction in compressive strength after 168 freeze-thaw cycles (%) and open porosity (%).

considered unsuitable for exterior utilisations owing to its water solubility, certain qualifications to this assertion are in order. Historically, alabaster has been employed as a surrogate for glass in façades, attributed to its inherent translucency. Distinctly, alabaster does not succumb to the same magnitude of mass erosion when positioned vertically (where rainwater washes it) as it does when laid horizontally as flooring. This is primarily due to its prolonged submersion in water when used horizontally, culminating in dissolution and augmented mass loss. Consequently, it is prudent to annotate within this research that alabaster, when arrayed vertically, may be viable for exterior applications, albeit with the assumption of progressive mass loss over time.

4. Conclusions

The appropriate selection of natural stone for exterior applications, particularly in environments prone to freeze-thaw cycles, is of vital importance. Enhanced understanding of the characteristics and behaviours of natural stones will broaden the available information, thereby aiding in informed decision-making regarding the most suitable applications for each type, ultimately enhancing the durability of the materials.

Due to the scarcity of comparative studies encompassing various natural stone families, the durability of the 14 primary building natural stone families against frost damage is analysed in this research, based on the capillary water absorption method. This method considers textural properties, open porosity, and compressive strength. The evaluation methodology proposed aims to adapt to stringent construction schedules, offering professionals in the sector an efficient alternative to the time-intensive freeze-thaw test. It is time-effective and capable of delivering relevant and precise data regarding the freeze-thaw durability of natural stones.

Through the relationship between various intrinsic properties and capillary water absorption, an accurate prediction of the potential damage from freeze-thaw cycles is established. The proven relationship between higher porosity values, also influenced by pore morphology, and the increase in water absorption in the stone (both total and capillary) is taken as a starting point. Consequently, the greater the water absorption, the more susceptible the stone is to damage from freeze-thaw cycles. Thus, the main conclusions of the research are as follows:

- The use of natural stones with an open porosity exceeding 2 % is not advisable for exterior applications where there is a potential for frost damage. In cases where the open porosity is greater than 2 %, the natural stones studied in this research demonstrated losses in

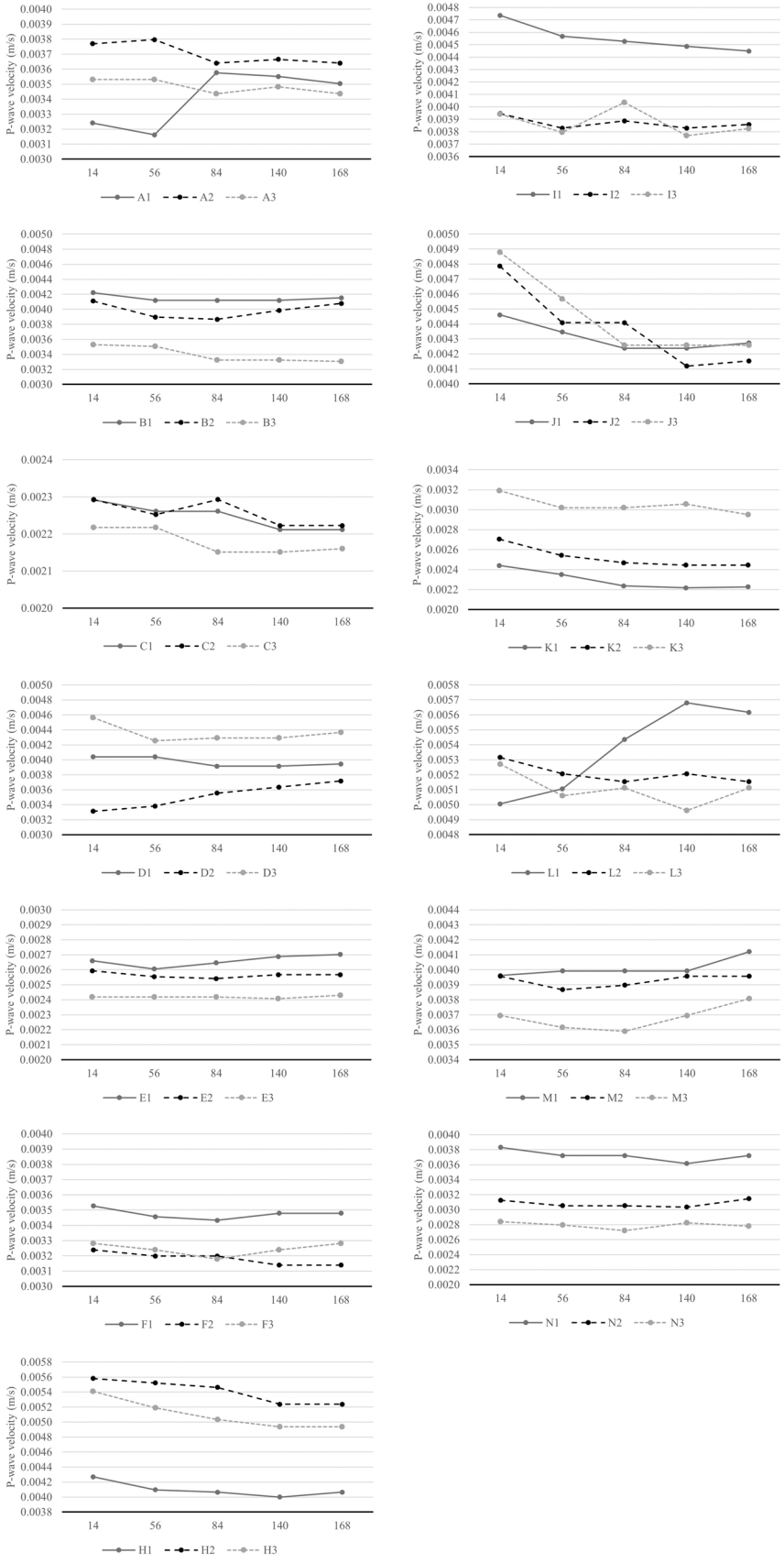

Fig. 8. P-wave velocity (m/s) of the samples during FT test, after 14–56-84–140-168 cycles.

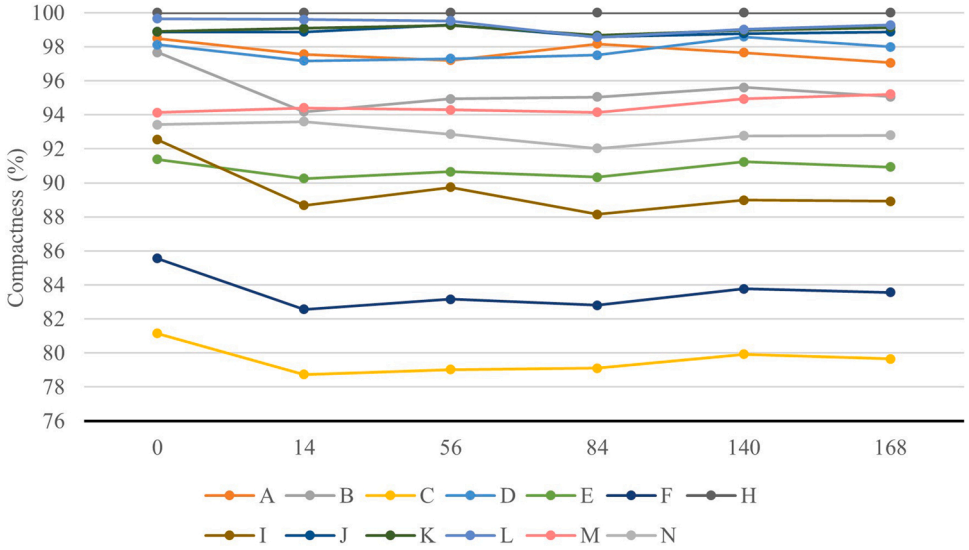

Fig. 9. Compactness (%) of the samples: initial and subsequent to 14–56-84–140-168 FT cycles.

compressive strength after 168 freeze-thaw cycles exceeding 10 % of their initial values. This finding is congruent with a criterion of capillary water absorption exceeding 600 g/m^2 after approximately 24 hours. This constraint on exterior application is predominantly pertinent to usage as flooring. Conversely, in instances of vertical cladding, the compressive strength assumes a diminished level of criticality. Moreover, when the natural stone is oriented vertically, its capacity to absorb water is notably less compared to a horizontal placement (as in flooring), where it can remain submerged for an extended period of time. Consequently, the utilisation of natural stone in outdoor applications (vertical cladding) is deemed considerably less restrictive.

- Behaviour deviating from this general trend is noted in certain natural stones, notably slate and travertine. Travertine, despite not absorbing as much water as other stones with greater compressive strength losses, is vulnerable due to its large cavities. The freezing of even small amounts of water within these cavities can cause significant damage and reduction in strength. Generally, it can be deduced that stones with finer porosity are more resistant to freeze-thaw cycles compared to those with larger porosity. Slate represents a unique case; although it has one of the lowest water absorptions, it undergoes significant loss in compressive strength. This is attributed to its foliated structure, where the small amount of water that does penetrate and then freezes can easily separate and break the layers through indirect traction in their plane, as they are not bonded with the rest of the layers.
- The P-wave velocity in most of the samples decreases as the number of freeze-thaw cycles increases, suggesting progressive damage. However, the data does not provide definitive information, largely due to the small size of the samples (50 mm).
- In analysing the behaviour of water expansion upon freezing, two key factors must be considered: the structure of the material and the environmental context. The risk associated with freeze-thaw cycles depends on the water absorption capacity of the materials, which is influenced by their location in the construction and their intrinsic properties. From an architectural perspective, the visual appearance of most natural stones does not significantly degrade after 168 freeze-thaw cycles. This holds true except for those stones characterized by large porosity and a heterogeneous porous morphology, which are more susceptible to visible deterioration.

The estimation of a natural stone's durability against freeze-thaw cycles can effectively be conducted through a capillary water absorption test and a porosity study. This methodology presents a considerable advantage in terms of reduced time and material costs. However, it is crucial to have a thorough understanding of the textural properties and mineralogical composition of the natural stone for accurate interpretation. This understanding is particularly important in the context of exceptional cases such as slate or travertine. Additionally, it is essential to acknowledge the inherent variability in natural materials; consequently, stones sourced from proximate locations may exhibit differing properties and yield varied results.

Funding sources

This research did not receive any specific grant from funding agencies in the public, commercial, or not-for-profit sectors.

CRediT authorship contribution statement

Jose Vercher: Writing – review & editing, Validation, Supervision, Software, Resources, Methodology, Investigation, Data curation, Conceptualization. **Carlos Lerma:** Writing – review & editing, Software, Formal analysis. **Júlia G. Borràs:** Writing – original draft, Visualization, Validation, Investigation, Formal analysis, Data curation. **Ángeles Mas:** Writing – review & editing, Resources, Methodology. **Enrique Gil:** Resources, Formal analysis, Conceptualization.

Declaration of Competing Interest

The authors declare that they have no known competing financial interests or personal relationships that could have appeared to influence the work reported in this paper.

Data Availability

Data will be made available on request.

Acknowledgements

Funding for open access charge: CRUE-Universitat Politècnica de València.

The authors express their sincere gratitude to R. Molina and D. Panal, laboratory technicians, for their invaluable assistance and support during the experimental procedures. They also extend their appreciation to Y. Ouahabi and A. Gil, students of the Bachelor's Degree in the

Fundamentals of Architecture at the Universitat Politècnica de València, for their collaboration in conducting the tests and data collection.

Furthermore, the authors wish to acknowledge the generous contribution of various quarries (Levantina, Olnasa, Arastone, and Cupa Pizarra) for providing the samples used in this study, as well as for their exceptional support and cooperation.

Declaration of interest statements

The authors report there are no competing interests to declare.

References

[1] A. Jamshidi, M.R. Nikudel, M. Khamehchiyan, Predicting the long-term durability of building stones against freeze–thaw using a decay function model, Cold Reg. Sci. Technol. 92 (2013) 29–36, https://doi.org/10.1016/j.coldregions.2013.03.007.
[2] W. Domaslowski, La conservation préventive de la Pierre (Ed), Unesco, Paris, 1982.
[3] Z. Rusin, P. Świercz, Frost resistance of rock materials, Constr. Build. Mater. 148 (2017) 704–714, https://doi.org/10.1016/j.conbuildmat.2017.04.198.
[4] S. Huang, S. Yu, Y. Ye, Z. Ye, A. Cheng, Pore structure change and physico-mechanical properties deterioration of sandstone suffering freeze-thaw actions, Constr. Build. Mater. 330 (2022) 127200, https://doi.org/10.1016/j.conbuildmat.2022.127200.
[5] J. Eslami, C. Walbert, A.-L. Beaucour, A. Bourges, A. Noumowe, Influence of physical and mechanical properties on the durability of limestone subjected to freeze-thaw cycles, Constr. Build. Mater. 162 (2018) 420–429, https://doi.org/10.1016/j.conbuildmat.2017.12.031.
[6] T.C. Chen, M.R. Yeung, N. Mori, Effect of water saturation on deterioration of welded tuff due to freeze-thaw action, Cold Reg. Sci. Technol. 38 (2004) 127–136, https://doi.org/10.1016/j.coldregions.2003.10.001.
[7] M.J. Setzer, Action of frost and deicing chemicals: Basic phenomena and testing, in: J. Marchand, M. Pigeon, M.J. Setzer (Eds.), Freeze-Thaw Durability of Concrete, CRC Press, London, 1997, pp. 1–20, https://doi.org/10.1201/9781482271553.
[8] J. Ruedrich, D. Kirchner, S. Siegesmund, Physical weathering of building stones induced by freeze–thaw action: a laboratory long-term study, Environ. Earth Sci. 63 (2011) 1573–1586, https://doi.org/10.1007/s12665-010-0826-6.
[9] H. Jia, S. Ding, Y. Wang, F. Zi, Q. Sun, G. Yang, An NMR-based investigation of pore water freezing process in sandstone, Cold Reg. Sci. Technol. 168 (2019) 102893, https://doi.org/10.1016/j.coldregions.2019.102893.
[10] F. Meng, Y. Zhai, Y. Li, R. Zhao, Y. Li, H. Gao, Research on the effect of pore characteristics on the compressive properties of sandstone after freezing and thawing, Eng. Geol. 286 (2021) 106088, https://doi.org/10.1016/j.enggeo.2021.106088.
[11] M. Hori, H. Morihiro, Micromechanical analysis on deterioration due to freezing and thawing in porous brittle materials, Int. J. Eng. Sci. 36 (4) (1998) 511–522, https://doi.org/10.1016/S0020-7225(97)00080-3.
[12] F. Bayram, Predicting mechanical strength loss of natural stones after freeze–thaw in cold regions, Cold Reg. Sci. Technol. 83-84 (2012) 98–102, https://doi.org/10.1016/j.coldregions.2012.07.003.
[13] A. Tuğrul, The effect of weathering on pore geometry and compressive strength of selected rock types from Turkey, Eng. Geol. 75 (2004) 215–227, https://doi.org/10.1016/j.enggeo.2004.05.008.
[14] J. Li, R.B. Kaunda, K. Zhou, Experimental investigations on the effects of ambient freeze-thaw cycling on dynamic properties and rock pore structure deterioration of sandstone, Cold Reg. Sci. Technol. 154 (2018) 133–141, https://doi.org/10.1016/j.coldregions.2018.06.015.
[15] R.M. Esbert, R.M. Marcos, J. Ordaz, M. Montoto, F.J. Alonso, L.M.S. del Rio, V.G. R. de Argandoña, L. Calleja, A.R. Rey, Petrografía, propiedades físicas y durabilidad de rocas utilizadas en el patrimonio monumental de Cataluña, España (2.ª parte), Mater. Constr. 41 (222) (1991) 49–59, https://doi.org/10.3989/mc.1991.v41.i222.745.
[16] J. García-Talegón, A.C. Iñigo, R. Sepúlveda, E. Azofra, Effect of artificial freeze-thaw and thermal shock ageing, combined or not with salt crystallisation on the colour of Zamora building stones (Spain), ChemEngineering 6 (2022) 61, https://doi.org/10.3390/chemengineering6040061.
[17] J. Ordaz, R.M. Esbert, Glosario de términos relacionados con el deterioro de las piedras de construcción, Mater. Constr. 38 (209) (1988) 39–45, https://doi.org/10.3989/mc.1988.v38.i209.847.
[18] J.E. Lindqvist, U. Åkesson, K. Malaga, Microstructure and functional properties of rock materials, Mater. Charact. 58 (2007) 1183–1188, https://doi.org/10.1016/j.matchar.2007.04.012.
[19] M. Deprez, T. De Kock, G. De Schutter, V. Cnudde, The role of ink-bottle pores in freeze-thaw damage of oolithic limestone, Constr. Build. Mater. 246 (2020) 118515, https://doi.org/10.1016/j.conbuildmat.2020.118515.
[20] H. Jia, S. Ding, Y. Wang, F. Zi, Q. Sun, G. Yang, An NMR-based investigation of pore water freezing process in sandstone, Cold Reg. Sci. Technol. 168 (2019) 102893, https://doi.org/10.1016/j.coldregions.2019.102893.
[21] A. Al-Omari, K. Beck, X. Brunetaud, Á. Török, M. Al-Mukhtar, Critical degree of saturation: A control factor of freeze–thaw damage of porous limestones at Castle of Chambord, France, Eng. Geol. 185 (2015) 71–80, https://doi.org/10.1016/j.enggeo.2014.11.018.
[22] X. Tan, W. Chen, J. Yang, J. Cao, Laboratory investigations on the mechanical properties degradation of granite under freeze–thaw cycles, Cold Reg. Sci. Technol. 68 (2011) 130–138, https://doi.org/10.1016/j.coldregions.2011.05.007.
[23] M. Mutlutürk, R. Altindag, G. Türk, A decay function model for the integrity loss of rock when subjected to recurrent cycles of freezing–thawing and heating–cooling, Int. J. Rock. Mech. Min. Sci. 41 (2004) 237–244, https://doi.org/10.1016/S1365-1609(03)00095-9.
[24] H. Yavuz, R. Altindag, S. Sarac, I. Ugur, N. Sengun, Estimating the index properties of deteriorated carbonate rocks due to freeze–thaw and thermal shock weathering, Int. J. Rock. Mech. Min. Sci. 43 (2006) 767–775, https://doi.org/10.1016/j.ijrmms.2005.12.004.
[25] D.T. Nicholson, F.H. Nicholson, Physical deterioration of sedimentary rocks subjected to experimental freeze-thaw weathering, Earth Surf. Process. Landf. 25 (2000) 1295–1307, https://doi.org/10.1002/1096-9837(200011)25:12%3C1295::AID-ESP138%3E3.0.CO;2-E.
[26] A. Rojo, F.J. Alonso, R.M. Esbert, Hydric properties of some iberian ornamental granites with different superficial finishes: a petrophysical interpretation, Mater. Constr. 53 (2003) 61–72, https://doi.org/10.3989/mc.2003.v53.i269.268.
[27] Z. Rusin, P. Świercz, Z. Owsiak, Effect of microstructure on frost durability of rock in the context of diagnostic needs, Procedia Eng. 108 (2015) 177–184, https://doi.org/10.1016/j.proeng.2015.06.134.
[28] R.M. Esbert, R.M. Marcos, J. Ordaz, M. Montoto, F.J. Alonso, L.M.S. del Rio, V.G. R. de Argandoña, L. Calleja, F.J. Alonso, A.R. Rey, Petrografía, propiedades físicas y durabilidad de algunas rocas utilizadas en el patrimonio monumental de Cataluña, España, Mater. Constr. 39 (214) (1989) 37–47, https://doi.org/10.3989/mc.1989.v39.i214.808.
[29] V. Cnudde, W. De Boever, J. Dewanckele, T. De Kock, M. Boone, M.N. Boone, G. Silversmit, L. Vincze, E. Van Ranst, H. Derluyn, S. Peetermans, J. Hovind, P. Modregger, M. Stampanoni, K. De Buysser, G. De Schutter, Multi-disciplinary characterization and monitoring of sandstone (Kandla Grey) under different external conditions, Q. J. Eng. Geol. Hydrogeol. 46 (2013) 95–106, https://doi.org/10.1144/qjegh2012-005.
[30] I. Tomašić, D. Lukić, N. Peček, A. Kršinić, Dynamics of capillary water absorption in natural stone, Bull. Eng. Geol. Environ. 70 (2011) 673–680, https://doi.org/10.1007/s10064-011-0355-x.
[31] M. Heidari, A.A. Momeni, B. Rafiei, S. Khodabakhsh, M. Torabi-Kaveh, Relationship between petrographic characteristics and the engineering properties of jurassic sandstones, Hamedan, Iran, Rock. Mech. Rock. Eng. 46 (2013) 1091–1101, https://doi.org/10.1007/s00603-012-0333-z.
[32] Ö. Eren, M. Bahali, Some engineering properties of natural building cut stones of Cyprus, Constr. Build. Mater. 19 (2005) 213–222, https://doi.org/10.1016/j.conbuildmat.2004.05.011.
[33] V. Amirkiyaei, E. Ghasemi, L. Faramarzi, Estimating uniaxial compressive strength of carbonate building stones based on some intact stone properties after deterioration by freeze–thaw, Environ. Earth Sci. 80 (2021) 352, https://doi.org/10.1007/s12665-021-09658-8.
[34] Asociación Española de Normalización y Certificación (AENOR), UNE-EN 1936. Métodos de ensayo para piedra natural. Determinación de la densidad real y aparente y de la porosidad abierta y total, 2007.
[35] Asociación Española de Normalización y Certificación (AENOR), UNE-EN 1925. Métodos de ensayo para piedra natural. Determinación del coeficiente de absorción de agua por capilaridad, 1999.
[36] Y. Ozcelik, A. Ozguven, Water absorption and drying features of different natural building stones, Constr. Build. Mater. 63 (2014) 257–270, https://doi.org/10.1016/j.conbuildmat.2014.04.030.
[37] Asociación Española de Normalización y Certificación (AENOR), UNE-EN 12371. Métodos de ensayo para piedra natural. Determinación de la resistencia a la heladicidad, 2011.
[38] Asociación Española de Normalización y Certificación (AENOR), UNE-EN 1926. Métodos de ensayo para la piedra natural. Determinación de la resistencia a la compresión uniaxial, 2007.
[39] J. Martínez-Martínez, D. Benavente, M. Gomez-Heras, L. Marco-Castaño, M.Á. García-del-Cura, Non-linear decay of building stones during freeze–thaw weathering processes, Constr. Build. Mater. 38 (2013) 443–454, https://doi.org/10.1016/j.conbuildmat.2012.07.059.
[40] I. Uğur, H.Ö. Toklu, Effect of multi-cycle freeze-thaw tests on the physico-mechanical and thermal properties of some highly porous natural stones, Bull. Eng. Geol. Environ. 79 (2020) 255–267, https://doi.org/10.1007/s10064-019-01540-z.
[41] J.M. Remy, M. Bellanger, F. Homand-Etienne, Laboratory velocities and attenuation of P-waves in limestones during freeze-thaw cycles, Geophysics 59 (2) (1994) 176–315, https://doi.org/10.1190/1.1443586.
[42] L. Hua, N. Fujun, X. Zhi-ying, L. Zhanju, X. Jian, Acoustic experimental study of two types of rock from the Tibetan Plateau under the condition of freeze-thaw cycles, Sci. Cold Arid Reg. 4 (2011) 21, https://doi.org/10.3724/SP.J.1226.2012.00021.
[43] D. Draebing, M. Krautblatter, P-wave velocity changes in freezing hard low-porosity rocks: laboratory-based time-average model, Cryosphere 6 (2012) 1163–1174, https://doi.org/10.5194/tc-6-1163-2012.
[44] M. Darot, T. Reuschlé, Acoustic wave velocity and permeability evolution during pressure cycles on a thermally cracked granite, Int. J. Rock. Mech. Min. Sci. 37 (2000) 1019–1026, https://doi.org/10.1016/S1365-1609(00)00034-4.
[45] K. Malaga-Starzec, U. Åkesson, J.E. Lindqvist, B. Schouenborg, Microscopic and macroscopic characterization of the porosity of marble as a function of temperature and impregnation, Constr. Build. Mater. 20 (2006) 939–947, https://doi.org/10.1016/j.conbuildmat.2005.06.016.

[46] J. Martínez-Martínez, D. Benavente, M.A. García-del-Cura, Spatial attenuation: the most sensitive ultrasonic parameter for detecting petrographic features and decay processes in carbonate rocks, Eng. Geol. 119 (2011) 84–95, https://doi.org/10.1016/j.enggeo.2011.02.002.
[47] C. Alves, C.A.M. Figueiredo, J. Sanjurjo-Sánchez, A.C. Hernández, Effects of water on natural stone in the built environment – A review, Geosciences 11 (2021) 459, https://doi.org/10.3390/geosciences11110459.
[48] M.K. Kovářová, Prague's winter climatic conditions – A case study of sandstone weathering, Proc. Int. Multidiscip. Sci. GeoConference: SGEM (2012) 265–270.
[49] H. Yavuz, Effect of freeze–thaw and thermal shock weathering on the physical and mechanical properties of an andesite stone, Bull. Eng. Geol. Environ. 70 (2011) 187–192, https://doi.org/10.1007/s10064-010-0302-2.